Local Performance Analysis of Uncertain Polynomial Systems with Applications to Actuator Saturation

Abhijit Chakraborty, Peter Seiler and Gary J. Balas

***Abstract*— This paper considers the local performance analysis of uncertain polynomial systems. A method for estimating an upper bound of the local $L_2 \to L_2$ gain is presented. The gain upper bound condition is formulated in terms of a dissipation inequality that incorporates an integral quadratic constraint to model the uncertainty. For polynomial systems, the dissipation inequality can be verified using sum-of-squares optimizations. This approach is applied to systems with actuator position and rate limits. The effectiveness of the proposed method is demonstrated on two numerical examples.**

I. INTRODUCTION

Practical applications of feedback control systems involve actuator saturation with amplitude and rate limits. Such systems exhibit nonlinear behavior and are an important aspect when analyzing and synthesizing any feedback control system. Ignoring the effects of actuator saturation can lead to performance degradation and even instability. This is particularly critical for flight control systems. Fighter aircraft have high maneuverability requirements and are usually pushed to their operational limits. The effects of actuator saturation can be catastrophic when the aircraft is operating at the edge of its flight envelope. Saturation may cause pilot-induced oscillations leading to degraded performance and even out-of-control departure. In fact, pilot-induced oscillations due to saturation are the reason for the crash of a Grippen [3] and the YF-22 crash landing [6].

Several methods exist to analyze the stability of a linear system in feedback with a nonlinear element [14]. Circle and Popov criteria are commonly used among those methods [14]. The Circle criterion analyzes a linear time invariant (LTI) system in feedback with a memoryless, time-varying sector bounded static nonlinearity. The Popov criterion analyzes an LTI system with a memoryless, static sector-bounded nonlinearity. The Circle and Popov criteria are used in [8], [21] to estimate Lyapunov functions by solving Linear Matrix Inequality (LMI) conditions providing stability and performance guarantees for linear systems with actuator saturation. Another method, not involving Circle and Popov criteria, can be found in [7], where the saturated linear systems are analyzed by expressing the saturation function as a convex combination of piecewise linear functions.

A majority of the research on analyzing feedback control systems with actuator saturation assumes both the plant and the controller are linear. This is a restrictive modeling assumption, especially for flight control systems. As mentioned before, the aircraft is more likely to operate in saturation on the limits of the operational boundary. Assuming linear dynamics for an aircraft operating on the boundary of the flight envelope can lead to erroneous conclusions about the system. Analyzing nonlinear systems with saturated input is still an ongoing research problem. In [26], the controller synthesis problem was investigated for polynomial systems with saturating input employing the Control Lyapunov Function (CLF) approach. However, analysis tools for nonlinear systems in feedback with actuator saturation are not yet well-developed.

The work in this paper is motivated by the need for tools to analyze the performance of nonlinear systems in feedback with actuator saturation. The paper first derives the more general problem of estimating the local $L_2 \to L_2$ gain for a special class of uncertain nonlinear systems with polynomial vector fields. The local $L_2 \to L_2$ gain is estimated using a dissipation inequality that uses an integral quadratic constraint to incorporate the effect of the uncertainty. The dissipation inequality condition is solved via the Sums-of-Square (SOS) optimization framework. Solutions are computationally tractable for small to medium sized dynamical systems ($\leq 8-10$ states). The results are applied to a short period aircraft model with rate saturation. Finally, the conclusions and future work are given in Section V.

II. PROBLEM FORMULATION

Consider the feedback interconnection in Figure 1. The input-output equations associated with this interconnection are given by Equations 1 and 2.

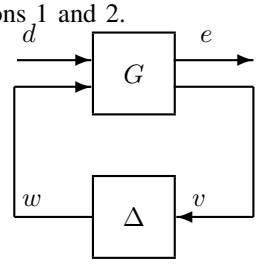

Fig. 1. Feedback Interconnection of $G - \Delta$

$$\begin{bmatrix} e \\ v \end{bmatrix} = G \begin{bmatrix} d \\ w \end{bmatrix} \tag{1}$$

$$w = \Delta(v) \tag{2}$$

In this setup, Δ is assumed to be a causal, bounded operator on L_2. G is a dynamical system expressed by polynomial

Abhijit Chakraborty is with Aerospace and Engineering Mechanics Department, University of Minnesota, chakrab@aem.umn.edu

Peter Seiler is with Aerospace and Engineering Mechanics Department, University of Minnesota, seiler@aem.umn.edu

Gary J. Balas is with Aerospace and Engineering Mechanics Department, University of Minnesota, balas@aem.umn.edu

vector fields of the following form:

$$\dot{x} = f(x, d, w) \tag{3}$$

$$\begin{bmatrix} e \\ v \end{bmatrix} = h(x) \tag{4}$$

where $x \in \mathbb{R}^n$ is the state vector, $d \in \mathbb{R}^{n_d}$ is the exogenous input, $e \in \mathbb{R}^{n_e}$ is the regulated output. $w \in \mathbb{R}^{n_w}$ and $v \in \mathbb{R}^{n_v}$ are the interconnection signals between G and Δ. Moreover, $f : \mathbb{R}^n \times \mathbb{R}^{n_d} \times \mathbb{R}^{n_w} \to \mathbb{R}^n$ and $h : \mathbb{R}^n \to \mathbb{R}^{n_e+n_v}$ are both multivariable polynomials. Assume $f(0,0,0) = 0$ and $h(0) = 0$. Note, h is not considered as a function of input w and d, i.e. G has no direct feedthrough from the inputs (d, w) to the outputs (e, v).

This paper is concerned with estimating the induced L_2 gain of the interconnection (Figure 1) from d to e. One issue is that the polynomial system G will not, in general, be globally stable. If the system is only locally stable then a sufficiently large disturbance can drive the state and the output of the system unbounded. Hence, the notion of local L_2 gain is introduced where attention is restricted to "local" inputs d that satisfy $||d||_2 \leq R$ where $R \in \mathbb{R}_+$. Formally, the local L_2 gain is defined in Equation 5.

$$\gamma_R := \sup_{\substack{d \in L_2, ||d||_2 \leq R \\ x(0)=0}} \frac{||e||_2}{||d||_2} \tag{5}$$

Computing the exact input-to-output gain γ_R for nonlinear systems is a challenging problem. Instead, we will be interested in estimating lower and upper bounds of the gain. Lower bounds will be computed using the method of [28] and this paper will derive conditions to compute upper bounds.

III. Local $L_2 \to L_2$ Gain Analysis

This section provides an approach to estimate an upper bound on the local L_2 energy gain. The approach is divided into three steps. First, the operator Δ is modeled using the Integral Quadratic Constraint (IQC) framework [17], [18]. Second, a dissipation inequality is formulated which provides a condition to estimate the local L_2 energy gain bound [12]. Finally, a computational approach is proposed using the Sum-of-Squares (SOS) framework in Section III-C.

A. Review of IQCs

IQCs, introduced in [18], provide a general framework for robustness analysis of linear dynamical systems with respect to uncertainties or nonlinearities. IQCs are used to constrain the input-output behavior of the uncertainties or nonlinearities. It is required that Δ be a bounded, causal operator which maps from $L_2 \to L_2$.

Let $\Pi : j\mathbb{R} \to \mathbb{C}^{(n_v+n_w)\times(n_v+n_w)}$ be a measurable, bounded Hermitian-valued function. Δ is said to satisfy the IQC defined by Π, if for all $v \in L_2$, with $w = \Delta(v)$, the following inequality holds [18],

$$\int_{-\infty}^{\infty} \begin{bmatrix} \hat{v}(j\omega) \\ \hat{w}(j\omega) \end{bmatrix}^* \Pi(j\omega) \begin{bmatrix} \hat{v}(j\omega) \\ \hat{w}(j\omega) \end{bmatrix} d\omega \geq 0 \tag{6}$$

where $\hat{v}(j\omega)$ and $\hat{w}(j\omega)$ are Fourier transforms of v and w, respectively. If the IQC multiplier Π is rational and uniformly bounded on the imaginary axis, then Equation 6 has an equivalent time domain expression. In that case, Π can be factorized as, $\Pi(jw) = \Psi(jw)^* M \Psi(jw)$, where M is a constant matrix and $\Psi(s)$ is a stable Linear Time Invariant (LTI) filter. The time domain interpretation of the IQC in Equation 6 can be formulated as [18]:

$$\int_0^{\infty} y_\psi(t)^T M y_\psi(t) dt \geq 0 \tag{7}$$

where y_Ψ is the output of the following state-space realization (See Figure 2).

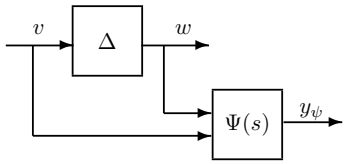

Fig. 2. Time Domain Interpretation of IQCs

$$\dot{x}_\Psi(t) = A_\Psi x_\Psi + B_{\Psi 1} v + B_{\Psi 2} w \tag{8}$$

$$y_\Psi(t) = C_\Psi x_\Psi + D_{\Psi 1} v + D_{\Psi 2} w \tag{9}$$

$$x_\Psi(0) = 0 \tag{10}$$

Moreover, Δ is said to satisfy the "hard" IQC defined by Π if,

$$\int_0^T y_\psi(t)^T M y_\psi(t) dt \geq 0 \quad \forall\, T < \infty \tag{11}$$

Δ is said to satisfy the "soft" IQC defined by Π if it is not "hard", i.e. if the time domain quadratic constraint does not hold for all finite time intervals T. The notions of "soft" and "hard" depend on the factorization of Π [24]. The dissipation inequality condition derived in this paper assumes that the "hard" conditions hold, i.e. the time-domain IQC condition is valid over all finite time intervals.

B. Local Dissipation Inequality Formulation

This section develops a dissipation inequality for estimating a local L_2 energy gain bound for the interconnection in Figure 1. The knowledge of Δ is incorporated in the dissipation inequality via an IQC representation of Δ. The main result for formulating the dissipation inequality is based on the connection between IQC theory and dissipation theory shown in [12], [24]. This connection [12], [24] is established for the special class of "hard" IQC factorizations.

Figure 3 shows the analysis interconnection structure which is obtained by simply replacing the relation $w = \Delta(v)$ with the time domain IQC constraint, $\int_0^T y_\psi(t)^T M y_\psi(t) dt \geq 0$. This interconnection is used to formulate the dissipation inequality provided in Theorem 1. For notational simplicity, let, $\tilde{x} = \begin{bmatrix} x \\ x_\psi \end{bmatrix}$ and $F(\tilde{x}, w, d) = \begin{bmatrix} \dot{x} \\ \dot{x}_\psi \end{bmatrix}$.

Theorem 1: Assume the interconnection of G and Δ is well-posed and Δ satisfies the hard IQC defined by $\Pi = \Psi^* M \Psi$. If $\exists$ a smooth, continuously differentiable function $V : \mathbb{R}^{n_x+n_{x_\psi}} \to \mathbb{R}$ and real numbers $\gamma,\ \lambda > 0$ such that:

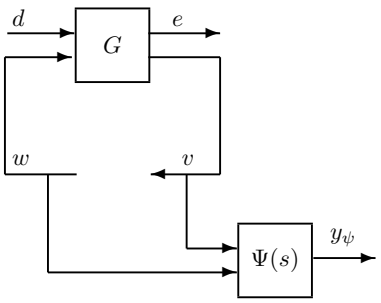

Fig. 3. Analysis Interconnection Structure

$$V(0) = 0 \text{ and } V(\tilde{x}) \geq 0 \ \ \forall \ \tilde{x} \tag{12}$$

$$\Omega_{V,R^2} := \{\tilde{x} : \ V(\tilde{x}) \leq R^2\}$$

$$\nabla V \cdot F(\tilde{x}, w, d) \leq d^T d - \frac{1}{\gamma^2} e^T e - \lambda(y_\psi^T M y_\psi)$$

$$\forall \tilde{x} \in \Omega_{V,R^2}, \forall d \in \mathbb{R}^{n_d} \text{ and } \forall w \in \mathbb{R}^{n_w} \tag{13}$$

then $||d||_2 < R$ implies $||e||_2 \leq \gamma ||d||_2$.

Proof: The theorem assumes the dissipation inequality holds only over a sublevel set, Ω_{V,R^2}. Hence, the proof first ensures that the state remains in the sublevel set for all finite time. Let $\tilde{x}(0) = 0$ and d be any input such that $||d||_2 < R$. Since the interconnection is assumed to be well-posed, unique solutions to the ODEs exist for all finite time. Assume $\exists$ a $T_1 > 0$ such that $x(T_1) \notin \Omega_{V,R^2}$. Define $T_2 := \inf_{x(T) \notin \Omega_{V,R^2}} T$. By continuity of the ODE solutions, $x(T_2) \in \partial\Omega_{V,R^2}$, where $\partial(\Omega_{V,R^2})$ indicates the boundary of the set Ω_{V,R^2}. We can conclude that $x(t) \in \Omega_{V,R^2}$ for all $t \in [0, \ T_2]$. Thus the dissipation inequality holds along the trajectory from $[0, \ T_2]$. Integrating this dissipation inequality gives:

$$\int_0^{T_2} \dot{V}(\tilde{x}) dt \leq \int_0^{T_2} (d^T d - \frac{1}{\gamma^2} e^T e) dt - \int_0^{T_2} \lambda(y_\psi^T M y_\psi) dt$$

Since the hard IQC satisfies $\int_0^{T_2} \lambda(y_\psi^T M y_\psi) dt \geq 0$ and $V(\tilde{x}(0)) = 0$, this inequality gives:

$$R^2 = V(\tilde{x}(T_2)) \leq \int_0^{T_2} d^T d \ dt \leq ||d||_2^2 < R^2$$

This is a contradiction and hence the assumption that $\exists$ a $T_1 > 0$ such that $x(T_1) \notin \Omega_{V,R^2}$ is not true. Thus $||d||_2 < R$ implies $x(t) \in \Omega_{V,R^2}$ for all finite time. Hence the dissipation inequality holds along the trajectories of $\tilde{x}$ for all finite time.

Integrating the dissipation inequality (Equation 13) from $t = 0$ to $t = T$ with the initial condition $\tilde{x}(0) = 0$ and using $V(\tilde{x}(0)) = 0$ and $V(\tilde{x}(T) \geq 0$ yields:

$$0 \leq \int_0^T \lambda(y_\psi^T M y_\psi) dt \leq \int_0^T (d^T d - \frac{1}{\gamma^2} e^T e) dt$$

This implies that $\frac{1}{\gamma^2} \int_0^T e^T e \ dt \leq \int_0^T d^T d \ dt$ for all finite time T and hence $||e||_2 \leq \gamma ||d||_2$. ■

Remark 1 Notice, $\frac{||e||_2}{||d||_2} \leq \gamma$ implies $\gamma_R \leq \gamma$. Hence, γ provides an upper bound estimate of the local L_2 gain.

Remark 2 The dissipation inequality formulated is restrictive in the sense that it is applicable only when hard factorization exists for the IQCs. Additionally, the theorem also requires the storage function to be positive definite. In [24], it was incorrectly claimed that this dissipation inequality condition is equivalent to the standard frequency domain IQC condition when G is restricted to be a linear system. The dissipation inequality condition in Theorem 1 is, for general multipliers, a more conservative condition than the standard frequency-domain IQC test. However, we are interested in polynomial G and the conservativeness of the bound is being investigated.

Remark 3 The operator Δ can be modeled as conic combinations of several multipliers. Hence, the term $\lambda(y_\psi^T M y_\psi)$ in the dissipation inequality can be replaced by $\sum_{i=1}^p \lambda_i(y_{\psi_i}^T M_i y_{\psi_i})$. Less conservative bounds on the L_2 gain will be computed if more IQCs are used.

C. Computation of $L_2 \rightarrow L_2$ Gain

This section turns the dissipation inequality conditions provided by Theorem 1 into a Sum-of-Squares (SOS) [15], [20] optimization problem. This is handled by relaxing the non-negativity of the original constraints with SOS constraints.

The dissipation inequality can be solved to estimate how the L_2 energy gain varies for different input size, R. There are two equivalent questions one may ask: (i) Given R such that $||d||_2 < R$, what is a tight upper bound for the induced $L_2 \rightarrow L_2$ gain γ , or (ii) Given the upper bound γ what is the largest value of R such that $||e||_2 \leq \gamma R$ whenever $||d||_2 < R$? We focus on answering the latter question.

The dissipation inequality (Equation 13) in Theorem 1 can be expressed as the following set containment condition:

$$\Omega_{V,R^2} \subset \{(\tilde{x}, w, d) : \nabla V \cdot F(\tilde{x}, w, d) \leq d^T d - \frac{1}{\gamma^2} e^T e - \lambda(y_\psi^T M y_\psi)\} \tag{14}$$

The set containment constraint in Equation 14 is replaced with a sufficient condition involving non-negative polynomials [2], [20] by applying generalized S-procedure, a simplification of the Positivstellensatz conditions.

$$-[(R^2 - V)s(\tilde{x}, w, d) + \nabla V \cdot F(\tilde{x}, w, d) - d^T d + \frac{1}{\gamma^2} e^T e + \lambda(y_\psi^T M y_\psi)] \geq 0 \tag{15}$$

where the function $s(\tilde{x}, w, d) \geq 0$ is a decision variable of the optimization, i.e. it is found as part of the optimization. If $s(\tilde{x}, w, d)$ and $V(\tilde{x})$ are restricted to be polynomial, both constraints involve the non-negativity of polynomial functions. The non-negativity conditions can be replaced by sufficient SOS constraints. Finally, the dissipation inequality conditions provided in Theorem 1 are reformulated as an SOS optimization problem, which can be solved by freely

available software [1], [16], [22], [25].

$$\begin{aligned}
&\bar{R} := \max R \\
&\quad \text{subject to:} \\
&V(\tilde{x}) \text{ is SOS}, V(0) = 0 && \text{(16a)} \\
&-[(R^2 - V)s(\tilde{x}, w, d) + \nabla V \cdot F(\tilde{x}, w, d) - d^T d \\
&\qquad + \frac{1}{\gamma^2} e^T e + \lambda(y_\psi^T M y_\psi)] \text{ is SOS} && \text{(16b)} \\
&\lambda > 0 && \text{(16c)} \\
&s(\tilde{x}, w, d) \text{ is SOS} && \text{(16d)}
\end{aligned}$$

Note, the optimization problem in Equation 16 is bilinear in decision variables. For example, the term $Vs(\tilde{x}, w, d)$ in Equation (16b) is bilinear in decision variable. If either V or s is fixed then the problem is quasiconvex and can be solved via bisection on R. Thus a V-s type iteration is proposed [9]–[11], [27] where V is solved for fixed s and vice versa. The storage function V in the iteration is initialized with the linearized storage function V_L by solving the following SOS condition.

$$-\nabla V_L \cdot F_L(\tilde{x}, w, d) - d^T d + \frac{1}{\gamma_L^2} e^T e + \lambda(y_\psi^T M y_\psi) \text{ is SOS}$$

where F_L represents the linearization of F and γ_L is the L_2 energy gain with $G = F_L$ in Figure 1. Now, the V-s iteration algorithm is applied for a given $\gamma > \gamma_L$. The V-s iteration steps are:

1) R^2/s **Step**: Hold V fixed and solve for s and $\bar{R}$

$$\begin{aligned}
&\bar{R} := \max R \\
&\quad \text{subject to:} \\
&\quad \text{Equation (16b) - (16d)}
\end{aligned}$$

2) V **step**: Hold $\bar{R}$, $s(\tilde{x}, w, d)$ fixed and solve for V satisfying Equation (16a) - (16c).
3) Repeat R^2/s and V step as long as the $\bar{R}$ continues to increase.

An interior-point linear matrix inequality solver is used in the SOS framework to find the solution to the above algorithm. Notice that the maximization of R in the R^2/s step is done independently of the feasibility search of the storage function in V step. There is no guarantee that the V step will provide a different storage function at each iteration step. It is possible to obtain the same storage function from the previous step. While this is possible, it typically happens that the solver returns a different V that allows R to be increased at the next iteration. This step can be understood by the fact that interior point solvers try to return a solution at the analytic center of set specified by the linear matrix inequality constraints. Thus the V step typically returns a feasible V that is "pushed away" from the constraints. A more formal theory for the behavior of this feasibility step is an open question.

IV. Applications

This section presents two examples involving estimation of the L_2 energy gain bound. The first example deals with the amplitude saturation and the second example is a flight control system with rate saturation.

A. Amplitude Saturation

Consider the feedback interconnection shown in Figure 1 with Δ denoting a normalized unit amplitude saturation function. The dynamics of G are given as:

$$\begin{aligned}
\dot{x}_1 &= -x_1 + x_2 + \alpha x_2^2 \\
\dot{x}_2 &= -x_2 + d + w \\
\begin{bmatrix} e \\ v \end{bmatrix} &= \frac{1}{2} \begin{bmatrix} x_1 \\ x_1 \end{bmatrix}
\end{aligned}$$

The normalized unit saturation function is given by:

$$\Delta(v) := \text{sat}(v) = \begin{cases} 1 & \text{if } v > 1 \\ v & \text{if } |v| \leq 1 \\ -1 & \text{if } v < -1 \end{cases} \qquad (17)$$

The goal is to estimate the upper bound of the $L_2 \to L_2$ gain from d to e for different values of α. The term α is a 'weighting' on the nonlinearity of the dynamics. For $\alpha = 0$, G reduces to a linear model. In that case, the L_2 gain from d to e can be computed by using the IQCβ [13] toolbox. The saturation is modeled as a $[0, 1]$ sector bounded nonlinearity. The L_2 gain computed with the IQCβ toolbox for the linear plant ($\alpha = 0$) is $\gamma = 1.0$. The gain bounds as α goes to zero will be compared with the linear analysis results obtained for $\alpha = 0$. The purpose of this example is to understand the conservatism introduced by the dissipation inequality condition.

The first step in analyzing the problem is to model the saturation in the IQC framework. This entails replacing the precise relation $w = \text{sat}(v)$ with the time domain IQC, $\int_0^T y_\psi(t)^T M y_\psi(t) dt \geq 0$. In this specific example, the $[0\ 1]$ sector bounded nonlinearity is considered, which satisfies the multiplier:

$$\Pi_1 = \begin{bmatrix} 0 & 1 \\ 1 & -2 \end{bmatrix} \qquad (18)$$

The dissipation inequality condition is solved to estimate the local L_2 gain for three different values of α. The L_2 gain is estimated with a quadratic storage function and the multiplier s is a quadratic function of $[x_1; x_2; w; d]$. Figure 4 shows that as α goes close to zero, the dissipation inequality recovers the linear results. Both the dissipation inequality

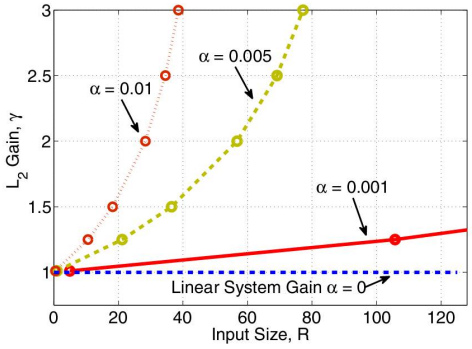

Fig. 4. L_2 gain bounds with quadratic storage function for different size of inputs and different values of α.

results for the nonlinear system and the linear results obtained by IQCβ could be improved by using additional IQCs. Several different Π's are known for amplitude saturation in literature [12]. The Popov IQC is one such multiplier.

B. Short Period Control with Rate Saturation

The L_2 gain estimation technique is applied to the NASA's Generic Transport Model (GTM) aircraft [5], [19] under rate saturation. A polynomial model of the GTM short period dynamics with pitch rate (q) feedback is considered. Details on the polynomial modeling can be found in [4].

Consider Figure 5. P is a two-state polynomial model of the GTM longitudinal-axis short-period dynamics. The states are $x := [\alpha \ q]$ where α is the angle of attack (rad) and q is the pitch rate (rad/s). A proportional pitch rate (q) feedback control law is considered and is denoted by K. Elevator deflection (δ_e in radian) is the control input. An exogenous disturbance d affects both states and enters into the plant additively. The goal is to estimate an upper bound of the local L_2 gain from d to $e = q$ under rate limit saturation. For simplicity, the rate limit in this example is designed to have a bandwidth of 1 rad/s. In reality, the GTM rate limit bandwidth is faster than 1 rad/s.

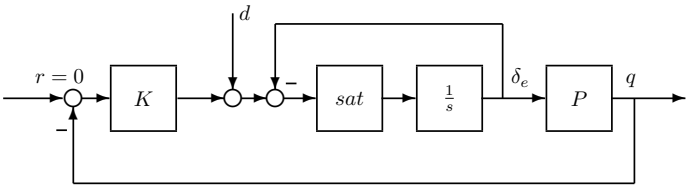

Fig. 5. Feedback interconnection of GTM short period dynamics

The polynomial short period model (P) is given by:

$$\begin{aligned}\dot{\alpha} &= -1.492\alpha^3 + 4.239\alpha^2 + 2.402 \times 10^{-1}\alpha\delta_e \\ &\quad + 3.063 \times 10^{-3}\alpha q - 6.491 \times 10^{-2}\delta_e^2 + 6.226 \times 10^{-3}q^2 \\ &\quad - 3.236\alpha - 3.166 \times 10^{-1}\delta_e + 9.227 \times 10^{-1}q \\ \dot{q} &= -7.228\alpha^3 + 18.36\alpha^2 + 41.50\alpha\delta_e - 45.34\alpha - 59.99\delta_e \\ &\quad - 4.372q\end{aligned}$$

The control law used in this example is $\delta_{e_{cmd}} := -Kq$, where $K = 4\frac{\pi}{180}$.

IQC Modeling of Rate Saturation: The first step is to model the rate limit saturation within the IQC framework. In the rate limiter, an integrator appears in combination with a saturation. This interconnection is not L_2 stable and hence the IQC framework cannot be used. However, [23] resolves this issue by encapsulating the nonlinearity in an artificial feedback loop, as shown in Figure 6. Let the feedback encapsulated rate limiter be denoted by $\tilde{\delta}_e = \Gamma_{\text{sat}}(\delta_{e_{cmd}})$. This is defined by the relations,

$$\begin{aligned}\dot{\delta}_e &= \text{sat}(\delta_{e_{cmd}} - \delta_e), \ \delta_e(0) = 0 \\ \tilde{\delta}_e &= \delta_e + \text{sat}(\delta_{e_{cmd}} - \delta_e)\end{aligned}$$

The following IQC multipliers are used to model the feedback encapsulated rate limit saturation, $\tilde{\delta}_e = \Gamma_{\text{sat}}(\delta_{e_{cmd}})$.

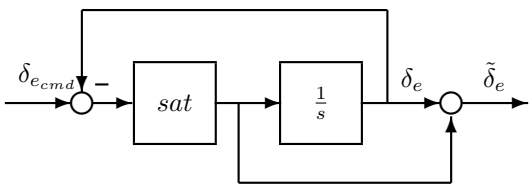

Fig. 6. Feedback encapsulation of rate limit

1) The gain from $\delta_{e_{cmd}}$ to $\tilde{\delta}_e$ is shown not to exceed $\sqrt{2}$ in [23]. This forms the basis of the following multiplier.
$$\Pi_{\Gamma_1} = \begin{bmatrix} 2 & 0 \\ 0 & -1 \end{bmatrix} \tag{19}$$
2) Another IQC multiplier can be derived by observing that the relation from $(\delta_{e_{cmd}} - \delta_e)$ to $\dot{\delta}_e$ can be modeled as a $[0, 1]$ sector bounded nonlinearity. The corresponding IQC multiplier is:
$$\Pi_{\Gamma_2} = \begin{bmatrix} 0 & \frac{j\omega}{j\omega+1} \\ (\cdot)^* & -2(\frac{j\omega}{j\omega+1})^*(\frac{j\omega}{j\omega+1}) \end{bmatrix} \tag{20}$$
3) Any conic combination of the above two multipliers are also considered as an appropriate IQC multiplier for the Γ_{sat} operator: $\Pi_\Gamma := \sum_{i=1}^{2} c_i \Pi_{\Gamma_i}$ for any $c_i \geq 0$ $(i = 1, 2)$

Remark Note the IQCs are provided for the encapsulated rate limiter, Γ_{sat}. Hence to use the IQCs for the encapsulated rate limit, an $(s + 1)$ filter is introduced at the output of the rate limit and a $\frac{1}{(s+1)}$ filter is introduced at the input of P. The feedback interconnection of $\tilde{P} = \frac{P}{s+1}$ and the encapsulated rate limit is then analyzed. The input-to-output gain from d to $e(= q)$ of this modified loop is equivalent to the d to e gain for the original problem.

The $L_2 \to L_2$ gain from d to q is estimated for the GTM dynamics under rate saturation. The rate saturation is modeled with a conic combination of the multipliers Π_{Γ_i} for $i = 1, 2$. The multiplier s is a quadratic function of $[\alpha; q; x_\Psi; \delta_e; d]$. x_Ψ is the state of the Ψ filter used in the factorization of Π_{Γ_2}. Figure 7 indicates how the induced gain of the system varies as the size of the disturbance $||d||_2$ increases. The horizontal axis indicates the size of the disturbance, $||d||_2$ and the vertical axis shows the estimated bounds of the induced gain from d to q. The upper bounds are estimated for both quadratic (marked as –x) and quartic (marked as -□) storage function. The induced gain for the linearized system is also shown (marked as --). The lower bound (marked as -o) is estimated using the algorithm proposed in [28]. The linear gain is estimated by solving the dissipation inequality for the linearized system and is computed to be 1.65. The quadratic and quartic storage function prove that the system can tolerate a disturbance input of size $||d||_2 < 0.4$ and $||d||_2 < 0.5$, respectively. The lower bound demonstrates that the system gain becomes unbounded for $||d||_2 < 1.83$. Note, for small $||d||_2$ the lower bound is below all three gains (linearized, quartic, quadratic). This is expected since the three gains are supposed to be upper bounds on the actual gain.

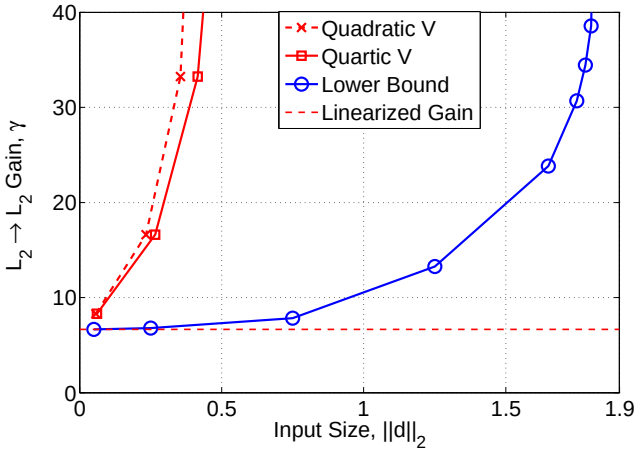

Fig. 7. Estimation of induced $L_2 - L_2$ gain bounds for GTM short period under rate limit

The upper bound results are conservative. The conservativeness is possibly due to the IQCs that are used for modeling rate saturation. The IQC in Equation 19 is constant and the other dynamic IQC in Equation 20 arises from modeling the saturation as sector bound nonlinearity. Research is underway to understand the appropriate use of dynamic IQCs to reduce conservatism.

V. Conclusion and Future Work

A method for estimating the upper bound of the induced L_2 gain for uncertain polynomial dynamical systems is presented. The method relies on merging the dissipation theory with the IQC framework. The SOS optimization framework has been used for computing the bounds. The technique has been applied for the case of saturation nonlinearity. Ultimately, the goal is to reduce the conservativeness of this method by including a rich description of IQCs. The framework will be extended to handle multiple nonlinearities. We also intend to quantify the conservativeness of the results by estimating the lower bound of the induced gain.

VI. Acknowledgements

This material is based upon work supported by the National Science Foundation under Grant No. 0931931 entitled "CPS: Embedded Fault Detection for Low-Cost, Safety-Critical System". Any opinions, fundings, and conclusions or recommendations expressed in this material are those of the author and do not necessarily reflect the views of the National Science Foundation. This research was also partially supported under the NASA Langley NRA Q7 contract NNH077ZEA001N entitled "Analytical Validation Tools for Safety Critical Systems." The technical contract monitor was Christine Belcastro.

References

[1] G. Balas, A. Packard, P. Seiler, and U. Topcu, "Robustness analysis of nonlinear systems," 2009, http://www.aem.umn.edu/∼AerospaceControl/.

[2] S. Boyd, L. E. Ghaoui, E. Feron, and V. Balakrishnan, *Linear Matrix Inequalities in System and Control Theory*. SIAM Studies in Applied Mathematics, 1994.

[3] P. Butterworth-Hayes, "Gripen crash raises canard fears," *Aerospace America*, vol. 32, pp. 10–11, February 1994.

[4] A. Chakraborty, P. Seiler, and G. J. Balas, "Nonlinear region of attraction analysis for flight control verification and validation," *Control Engineering Practice*, 2011, doi:10.1016/j.conengprac.2010.12.001.

[5] D. Cox, *The GTM DesignSim v0905*, 2009.

[6] M. Domheim, "Report pinpoints factors leading to YF-22 crash," *Aviation Week and Space Technology*, pp. 53–54, November 1992.

[7] H. Fang, Z. Lin, and T. Hu, "Analysis of linear systems in the presence of actuator saturation and L_2 disturbances," *Automatica*, vol. 40, pp. 1229 – 1238, 2004.

[8] H. Hindi and S. Boyd, "Analysis of linear systems with saturation using convex optimization," in *IEEE Conference on Decision and Control*, 1998, pp. 903 – 908.

[9] Z. Jarvis-Wloszek, "Lyapunov based analysis and controller synthesis for polynomial systems using sum-of-squares optimization," Ph.D. dissertation, University of California, Berkeley, 2003.

[10] Z. Jarvis-Wloszek, R. Feeley, W. Tan, K. Sun, and A. Packard, "Some controls applications of sum of squares programming," in *IEEE Conference on Decision and Control*, vol. 5, 2003, pp. 4676–4681.

[11] ——, *Positive Polynomials in Control*, ser. Lecture Notes in Control and Information Sciences. Springer-Verlag, 2005, vol. 312, ch. Controls Applications of Sum of Squares Programming, pp. 3–22.

[12] U. Jonsson, "Robustness analysis of uncertain and nonlinear systems," Ph.D. dissertation, Lund Institute of Technology, 1996.

[13] U. Jonsson, C. Y. Kao, A. Megretski, and A. Rantzer, *A Guide To IQCβ : A MATLAB Toolbox for Robust Stability and Performance Analysis*, Available from `http://people.eng.unimelb.edu.au/cykao`, 2004.

[14] H. Khalil, *Nonlinear Systems*, 2nd ed. Prentice Hall, 1996.

[15] J. Lasserre, "Global optimization with polynomials and the problem of moments," *SIAM Journal on Optimization*, vol. 11, no. 3, pp. 796–817, 2001.

[16] J. Lofberg, "Yalmip : A toolbox for modeling and optimization in MATLAB," in *Proceedings of the CACSD Conference*, Taipei, Taiwan, 2004. [Online]. Available: http://control.ee.ethz.ch/∼joloef/yalmip.php

[17] A. Megretski, "Kyp lemma for non-strict inequalities and the associated minimax theorem," 2010, eprint arXiv:1008.2552.

[18] A. Megretski and A. Rantzer, "System analysis via integral quadratic constraints," *IEEE Transactions on Automatic Control*, vol. 42, pp. 819 – 830, 1997.

[19] A. Murch and J. Foster, "Recent NASA research on aerodynamic modeling of post-stall and spin dynamics of large transport airplanes," in *45th AIAA Aerospace Sciences Meeting*, no. AIAA 2007-0463, 2007.

[20] P. Parrilo, "Structured semidefinite programs and semialgebraic geometry methods in robustness and optimization," Ph.D. dissertation, California Institute of Technology, 2000.

[21] C. Pittet, S. Tarbouriech, and C. Burgat, "Stability regions for linear systems with saturating controls via circle and Popov criteria," in *IEEE Conference on Decision and Control*, 1997, pp. 4518 – 4523.

[22] S. Prajna, A. Papachristodoulou, P. Seiler, and P. A. Parrilo, *SOSTOOLS: Sum of squares optimization toolbox for MATLAB*, Available from `http://www.cds.caltech.edu/sostools` and `http://www.mit.edu/∼parrilo/sostools`, 2004.

[23] A. Rantzer and A. Megretski, "Analysis of rate limiters using integral quadratic constraints," in *Proceedings of IFAC Nonlinear Control Systems Design Symposium*, 1998, pp. 696–700.

[24] P. Seiler, A. Packard, and G. Balas, "A dissipation inequality formulation for stability analysis with integral quadratic constraints," in *IEEE Conference on Decision and Control*, 2010, pp. 2304 – 2309.

[25] J. Sturm, "Using SeDuMi 1.02, a MATLAB toolbox for optimization over symmetric cones," *Optimization Methods and Software*, pp. 625–653, 1999.

[26] K. Sun, "Robust linear filter design via LMIs and controller design with actuator saturation via SOS programming," Ph.D. dissertation, University of California, Berkeley, 2008.

[27] W. Tan and A. Packard, "Searching for control Lyapunov functions using sums of squares programming," in *42nd Annual Allerton Conference on Communications, Control and Computing*, 2004, pp. 210–219.

[28] J. Tierno, R. Murray, and J. C. Doyle, “An efficient algorithm for performance analysis of nonlinear control systems,” in *Proceedings of the American Control Conference*, 1995, pp. 2717–2721.